

RESEARCH

Open Access



Targeting Src homology phosphatase 2 ameliorates mouse diabetic nephropathy by attenuating ERK/NF- κ B pathway-mediated renal inflammation

Che Yu^{1,2,3}, Zhuo Li¹, Cuili Nie⁴, Lei Chang¹ and Tao Jiang^{5*}

Abstract

Renal inflammation is a pivotal mechanism underlying the pathophysiology of diabetic nephropathy (DN). The Src homology phosphatase 2 (SHP2) has been demonstrated to be linked to diabetes-induced inflammation, yet its roles and explicit molecular mechanisms in DN remain unexplored. Here, we report that SHP2 activity is upregulated in both DN patients and db/db mice. In addition, pharmacological inhibition of SHP2 with its specific inhibitor PHP51 alleviates DN in db/db mice and attenuates renal inflammation. In vitro, PPHP51 administration prevents inflammatory responses in HK-2 cells stimulated by high glucose (HG). Mechanistically, PPHP51 represses HG-induced activation of the proinflammatory ERK/NF- κ B signaling pathway, and these inhibitory effects are blocked in the presence of an ERK specific inhibitor, hence demonstrating that PPHP51 suppresses ERK/NF- κ B pathway-mediated inflammation. Moreover, PPHP51 retards ERK/NF- κ B pathway activation in db/db mice, and histologically, SHP2 activity is positively correlated with ERK/NF- κ B activation in DN patients. Taken together, these findings identify SHP2 as a potential therapeutic target and show that its pharmacological inhibition might be a promising strategy to mitigate DN.

Keywords Diabetic nephropathy, Src homology phosphatase 2, ERK/NF- κ B pathway, Renal inflammation

Introduction

Diabetic nephropathy (DN) is the leading cause for the end-stage renal disease (ESRD), a common complication of diabetes mellitus (DM) [1]. The pathophysiological mechanisms of DN and induced kidney damage are poorly understood, and effective molecular targets to intervene disease progression are still lacking [2]. Despite current therapies for controlling hypertension, glycemic load and hyperlipidemia, a majority of DN patients progress to the stage of ESRD [3]. To date, the pathogenesis of DN has been closely associated with four causalities, including metabolic, hemodynamic, growth, and proinflammatory factors [4]. Increasing evidence has indicated that renal inflammation plays a central role in DN pathology via regulation of proinflammatory signaling pathways [5, 6]. Therefore, elucidating the molecular mechanisms

*Correspondence:

Tao Jiang

jtscri@163.com

¹ Department of Nephrology, Provincial Hospital Affiliated to Shandong First Medical University, Jinan, Shandong, China

² Postdoctoral Mobile Station of Shandong University, Jinan, Shandong, China

³ Medical Integration and Practice Center, Cheeloo College of Medicine, Shandong University, Jinan, Shandong, China

⁴ Division of Pediatrics Neurology, Provincial Hospital Affiliated to Shandong First Medical University, Jinan, Shandong, China

⁵ Department of Anesthesiology, Shandong Cancer Hospital and Institute, Shandong First Medical University and Shandong Academy of Medical Sciences, 440 Jiyan Road, Huaiyin District, Jinan 250117, Shandong, China



© The Author(s) 2023. **Open Access** This article is licensed under a Creative Commons Attribution 4.0 International License, which permits use, sharing, adaptation, distribution and reproduction in any medium or format, as long as you give appropriate credit to the original author(s) and the source, provide a link to the Creative Commons licence, and indicate if changes were made. The images or other third party material in this article are included in the article's Creative Commons licence, unless indicated otherwise in a credit line to the material. If material is not included in the article's Creative Commons licence and your intended use is not permitted by statutory regulation or exceeds the permitted use, you will need to obtain permission directly from the copyright holder. To view a copy of this licence, visit <http://creativecommons.org/licenses/by/4.0/>. The Creative Commons Public Domain Dedication waiver (<http://creativecommons.org/publicdomain/zero/1.0/>) applies to the data made available in this article, unless otherwise stated in a credit line to the data.

involved in inflammation-mediated DN progression and kidney injury may identify novel targets for developing preventive or curative therapies for DN.

The Src-homology domain-2-containing protein tyrosine phosphatase 2 (SHP2) is a cytosolic protein tyrosine phosphatase (PTP) expressed in most mammalian tissues and cells [7]. SHP2 is involved in the regulation of growth factor and cytokine signaling pathways, and its mutations account for genetic diseases in the cardiovascular system [8]. Moreover, studies have related SHP2 biological functions to inflammatory and diabetic conditions. For example, SHP2 mediates endothelial inflammation induced by chronic insulin through limiting NO production [9]. In addition, methylglyoxal accumulation induced by hyperglycaemia promotes the resistance of diabetic monocytes to VEGF through SHP2 activation [10]. Further, recent studies have reported that in diabetic patients, SHP2 activates aberrant activation of primary human monocytes [11], and repression of its activity impedes monocyte activation [12]. Despite these activities involved in diabetes-induced inflammation, less is known about whether SHP2 exerts an influence on DN progression and renal injury in diabetic patients and animal models.

In the present study, we took advantage of histologic examinations of human samples, a diabetic mouse model, as well as in vitro cellular studies, and provided some lines of evidence demonstrating that the SHP2 activity was augmented in human DN and db/db mice, as indicated by its elevated phosphorylated level, which promoted renal inflammation through downstream activation of the proinflammatory ERK/NF- κ B pathway. Most importantly, we also observed that in db/db mice, renal injury was alleviated by a pharmacological inhibition of SHP2 using its specific inhibitor PHPS1. These results support SHP2 to be a promising therapeutic target in DN treatment.

Materials and methods

Antibodies and reagents

Antibodies and reagents were provided from the following sources: phospho-SHP-2 (Tyr542) rabbit mAb, SHP-2 rabbit mAb, phospho-Erk1/2 (Thr202/Tyr204) rabbit mAb, Erk1/2 rabbit mAb, phospho-NF- κ B (Ser536) rabbit mAb and NF- κ B mouse mAb were obtained from Cell Signaling Technology; CCL-2 mouse mAb was purchased from Invitrogen; β -actin mouse mAb and F4/80 rat mAb were purchased from abcam; SHP2 specific inhibitor PHPS1 and ERK specific inhibitor PD98059 were purchased from Sigma-Aldrich.

Human kidney samples

Written informed consent was obtained from each patient prior to the sampling of kidney biopsy, which

were obtained from 14 patients with DN. Besides, 9 normal nephrectomy samples were used as controls.

Animal experiments

C57BLKS/J-leprdb/leprdb (db/db) mice and wild-type littermates (WT) were purchased from Nanjing Junke Bioengineering Co., Ltd. Mice were acclimatized to the feeding center for 2 weeks before use. Mice were classified into 4 groups ($n=6$) at 8 weeks of age, including groups of WT + PHPS1 and db/db + PHPS1 mice injected i.p. with PHPS1 (8 mg/kg body weight) and groups of WT + Ctrl and db/db + Ctrl mice injected i.p. with equal volume of vehicle. Mice were treated every day for 12 weeks. The blood glucose and body weight were measured every two weeks. A metabolic cage was used to collect the twenty-four-hour urine every 2 weeks. Urinary albumin and creatinine levels were determined by enzyme-linked immunosorbent assay (ELISA) kits (abcam). At 20 weeks of age, mice were sacrificed and blood and kidney tissue samples were harvested, which were stored for further usage. Serum creatinine levels in the blood samples were measured through QuantiChrom Aassay Kit (BioAssay Systems). Kidney samples were fixed in paraformaldehyde and embedded within paraffin or frozen in OCT. Tissue Sections with 4- μ m thickness were cut. Hematoxylin-eosin, Masson trichrome and periodic acid-Schiff staining was performed to assess renal injury. The intensity of injury was evaluated semiquantitatively by two independent researchers with a blinded manner using a scoring system described in previous studies [13, 14]. The positive immunostaining on kidney sections was semiquantified by Image-Pro Plus Software (Media Cybernetics), and the value was expressed as integrated optical density.

Cell culture

Human proximal tubular HK-2 cells were purchased from ATCC and cultured at 37°C in DMEM/F12 (Sigma-Aldrich) medium supplemented with 10% fetal bovine serum (Gibco), 1% penicillin/streptomycin in an atmosphere (5% CO₂, 95% air). Prior to treatment, HK-2 cells were cultured in serum-free medium for 12 h for starvation, followed by stimulation with 30 mmol/L of high glucose (Sigma-Aldrich) for further 24 h. The control group was cultured with 5.5 mmol/L glucose. HK-2 cells were pretreated with 5 μ M PHPS1 alone or in combination with 50 μ M PD98059 2 h before glucose stimulation.

qRT-PCR analysis

Total RNA from kidney tissues and HK-2 cells was isolated by TRIzol method (Invitrogen). Quantitative reverse transcription and PCR (qRT-PCR) analysis was

conducted by using an M-MLV Platinum RT-qPCR Kit (Invitrogen) and Eppendorf Real plex 4 instrument (Eppendorf). Specific primers for SHP2, TNF- α , IL-6, CCL-2 and β -actin were purchased from Sangon Biotech. Relative fold change of gene expression was calculated by $2^{-\Delta\Delta CT}$ method and normalized to that of β -actin.

Immunoblotting

The concentration of proteins of tissue and cell lysates was determined by Bradford method (Bio-Rad), and then separated by 10% sodium dodecyl sulfate-polyacrylamide gel electrophoresis (SDS-PAGE). Proteins were then transferred to polyvinylidene fluoride membranes (Bio-Rad), which were incubated at room temperature for 1 h in a blocking buffer (5% non-fat milk diluted in Tris-buffered saline containing 0.05% Tween 20). Membranes were probed with specific primary antibodies overnight at 4°C, and with secondary antibodies conjugated with horseradish peroxidase for another 1 h at room temperature. Immunoreactive bands on the membranes were visualized by enhanced chemiluminescence reagent (Bio-Rad).

Statistics

All data are expressed as the mean \pm SD. Statistical significance was calculated using Student's test or one-way ANOVA test followed by a Holm-Sidak post-test, as appropriate. All the statistical analyses was conducted with GraphPad Prism 6.0 software (San Diego, CA, USA). A p value less than 0.05 was considered statistically significant.

Results

SHP2 activity is enhanced in DN patients

To evaluate whether SHP2 is involved in DN pathogenesis, we conducted Western blot analysis to determine its activity (represented as the level of phosphorylated SHP2, p-SHP2) in kidney biopsy samples of DN patients, and normal kidney biopsy samples were used as controls. The result showed that the ratio of p-SHP2/SHP2 was markedly elevated in DN samples compared with that in normal controls (Fig. 1A), suggesting that SHP2 is activated in DN patients. Of note, we did not observe upregulation of basal expression level of SHP2 in DN patients, as shown by qRT-PCR analysis (Fig. 1B). To confirm these data, we performed immunostaining of p-SHP2 on DN samples through

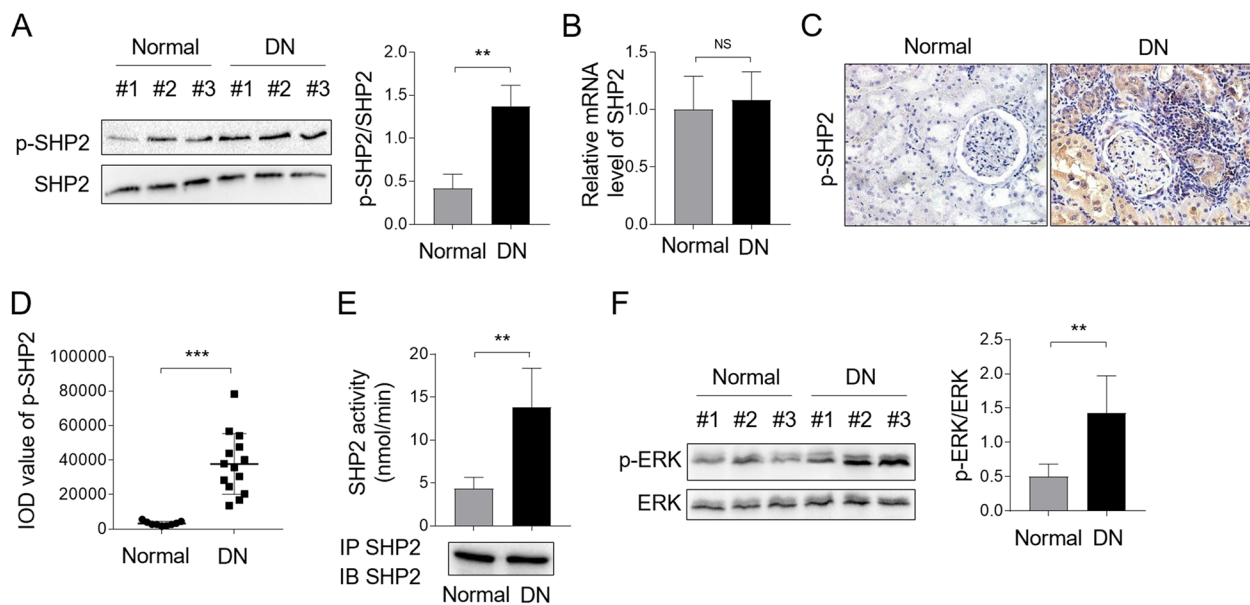


Fig. 1 SHP2 is activated in DN patients. **A** levels of p-SHP2 and basal SHP2 protein expression in DN kidney biopsies were measured by Western blot analysis. Normal kidney biopsies were used as control samples. The intensity of protein bands was quantified by ImageJ and the ratio of p-SHP2/SHP2 was shown right. Student's test, **, $p < 0.01$ ($n = 6$). **B** The mRNA level of SHP2 in DN and normal groups was checked by qRT-PCR analysis. The result relative to the normal group was depicted. Student's test, NS, not significant ($n = 6$). **C, D** Immunostaining of p-SHP2 on normal kidney sections ($n = 9$) and kidney biopsy samples of DN patients ($n = 14$) was visualized by IHC experiment (**C**). The integrated optical density (IOD) of p-SHP2 expression in (**C**) was shown (**D**). One-way ANOVA test followed by a Holm-Sidak post-test, ***, $p < 0.001$. **E** SHP2 immune complex PTP assay was performed using pNPP as a substrate on human DN samples ($n = 9$) and normal controls ($n = 6$). Immunoblotting control for immunoprecipitated SHP2 was shown below. One-way ANOVA test followed by a Holm-Sidak post-test, **, $p < 0.01$. **F** Levels of p-ERK and basal ERK protein expression in DN kidney biopsies were measured by Western blot analysis. Normal kidney biopsies were used as control samples. The intensity of protein bands was quantified by ImageJ and the ratio of p-ERK/ERK was shown right. Student's test, **, $p < 0.01$ ($n = 6$)

immunohistochemistry technique (IHC). As shown in Fig. 1C-D, p-SHP2 staining was notably enhanced in DN samples in comparison with normal kidney biopsies, showing predominantly cytosolic location. Moreover, we took advantage of an immune-complex phosphatase assay to measure SHP2 activity in kidney biopsy samples with DN, and found that SHP2 activity was indeed increased significantly (nearly 3.2-fold) in DN as compared with normal ones (Fig. 1E), further proving that SHP2 activity is strengthened in DN. SHP2 is well-established to ignite downstream activation of ERK mitogen-activated protein kinase in multiple pathways [15–17]. To confirm the activation of SHP2, we further checked the status of ERK in DN samples with an antibody probing ERK phosphorylation. As expected, consistent with SHP2 activation, the phosphorylated level of ERK (p-ERK) was also increased in DN in contrast to the normal group (Fig. 1F), suggesting an activated SHP2/ERK pathway in DN condition. Collectively, these results indicate that SHP2 is activated in DN patients, implying a potential role of SHP2 involved in DN pathogenesis.

SHP2 is activated in diabetic mice

We next used db/db mice, a murine model that recapitulates human DN [18], to investigate a potential connection of SHP2 to animal DN pathology. The blood glucose levels and body weight of mice were monitored, demonstrating typical changes in mice with DN compared to wild-type mice (Supplementary Fig. 1). Likewise, Western blot analysis showed that both the phosphorylation levels of SHP2 and downstream ERK were increased significantly in db/db mice, in contrast to wild-type mice (WT) (Fig. 2A), and the ratio of p-SHP2/SHP2 (Fig. 2B) and p-ERK/ERK (Fig. 2C) was also prominently increased in db/db mice. In agreement with these, IHC staining on kidney samples of mice also showed an overt upregulation of p-SHP2 in db/db mice (Fig. 2D). Consistent with these data, the immune-complex phosphatase assay uncovered that the activity of SHP2 in kidney samples from db/db mice was drastically augmented compared with that of WT mice (Fig. 2E). Hence, similar to those observations of human DN, the activity of SHP2 is also amplified in mouse DN model, together demonstrating an association of activated SHP2 with DN pathology.

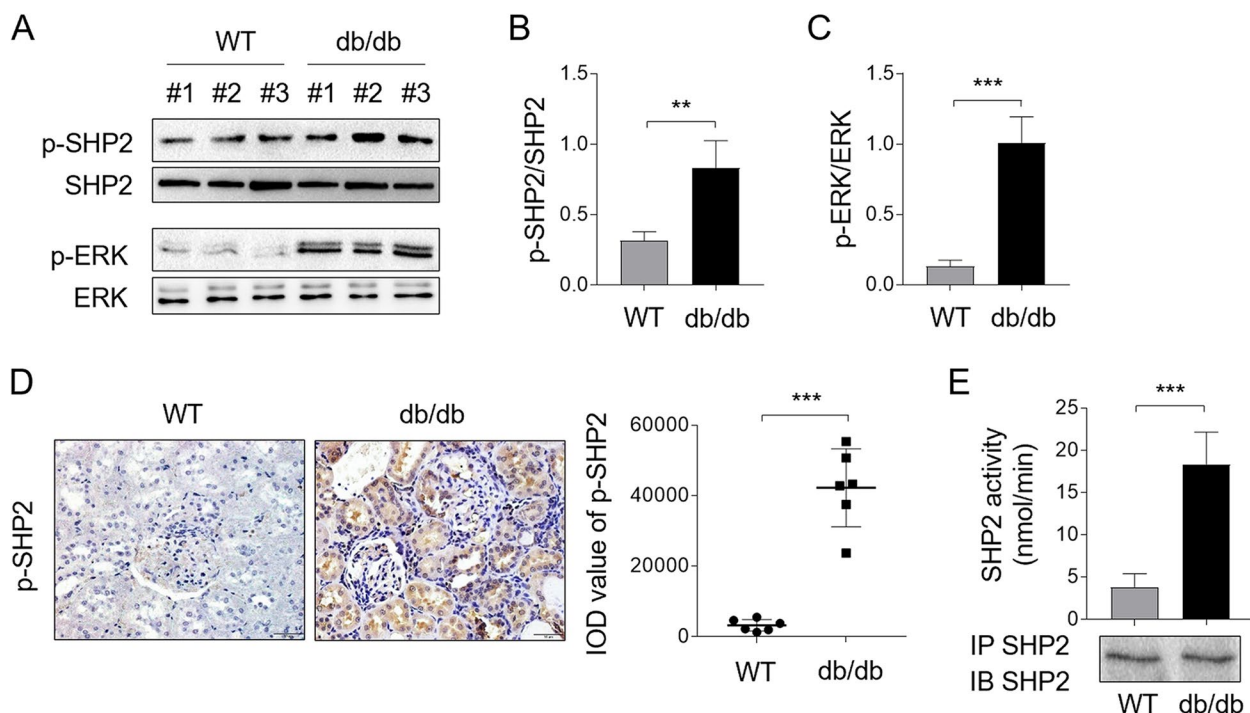


Fig. 2 SHP2 is activated in db/db mice. **A** Levels of p-SHP2, p-ERK and their basal protein expression in kidney biopsies of db/db mice were measured by Western blot analysis. Normal kidney biopsies of WT mice were used as control samples. **B, C** The intensity of protein bands (**A**) was quantified by ImageJ and the ratio of p-SHP2/SHP2 (**B**) and p-ERK/ERK (**C**) was shown right. Student’s test, **, $p < 0.01$; ***, $p < 0.001$ ($n = 6$). **D** Immunostaining of p-SHP2 on mouse normal kidney sections ($n = 6$) and kidney biopsy samples of db/db mice ($n = 6$) was detected by IHC experiment. The integrated optical density (IOD) of p-SHP2 expression was shown right. Student’s test, ***, $p < 0.001$. **E** SHP2 immune complex PTP assay was performed using pNPP as a substrate on normal kidney samples ($n = 6$) from WT mice and DN kidney samples from db/db mice ($n = 6$). Immunoblotting control for immunoprecipitated SHP2 was shown below. Student’s test, ***, $p < 0.001$

SHP2 inhibition with PHP51 alleviates renal injury in db/db mice

To explore a potential protective effect of counteracting SHP2 activation on renal injury in db/db mice, we utilized a pharmacological inhibition strategy in which PPHP51, a specific inhibitor of SHP2 [19], was administered by i.p. injection (8 mg/kg/day) to db/db mice for 12 weeks. Western blot analysis of the whole lysates of kidney tissue demonstrated an effective inhibition of SHP2 activation in db/db mice in the presence of PPHP51 administration, as shown by drastic decrease level of p-SHP2 (Fig. 3A). Additionally, PPHP51 treatment resulted in significant loss of kidney weight in db/db mice, without causing evident change in WT mice (Fig. 3B). Importantly, the levels of serum creatinine (Fig. 3C) and urine

albumin-to-creatinine ratio (UACR) (Fig. 3D) in db/db mice were sharply decreased upon PPHP51 treatment, while no obvious changes were observed in WT mice. Moreover, histological analyses of renal sections through PAS staining and hematoxylin and eosin (HE) staining displayed glomerulosclerosis, glomerular vascular tufts, atypical tubular epithelia and interstitial expansion in diabetic db/db mice, while these structural changes were reduced by PPHP51 treatment (Fig. 3E-F). Furthermore, increased fibrosis and collagen deposition in the interstitial compartment of kidneys from diabetic db/db mice were stained by Masson's trichrome, which was further verified by type I collagen (collagen-I) staining, indicating a significant increase of interstitial fibrosis and tubular atrophy (IFTA) in db/db mice, while these

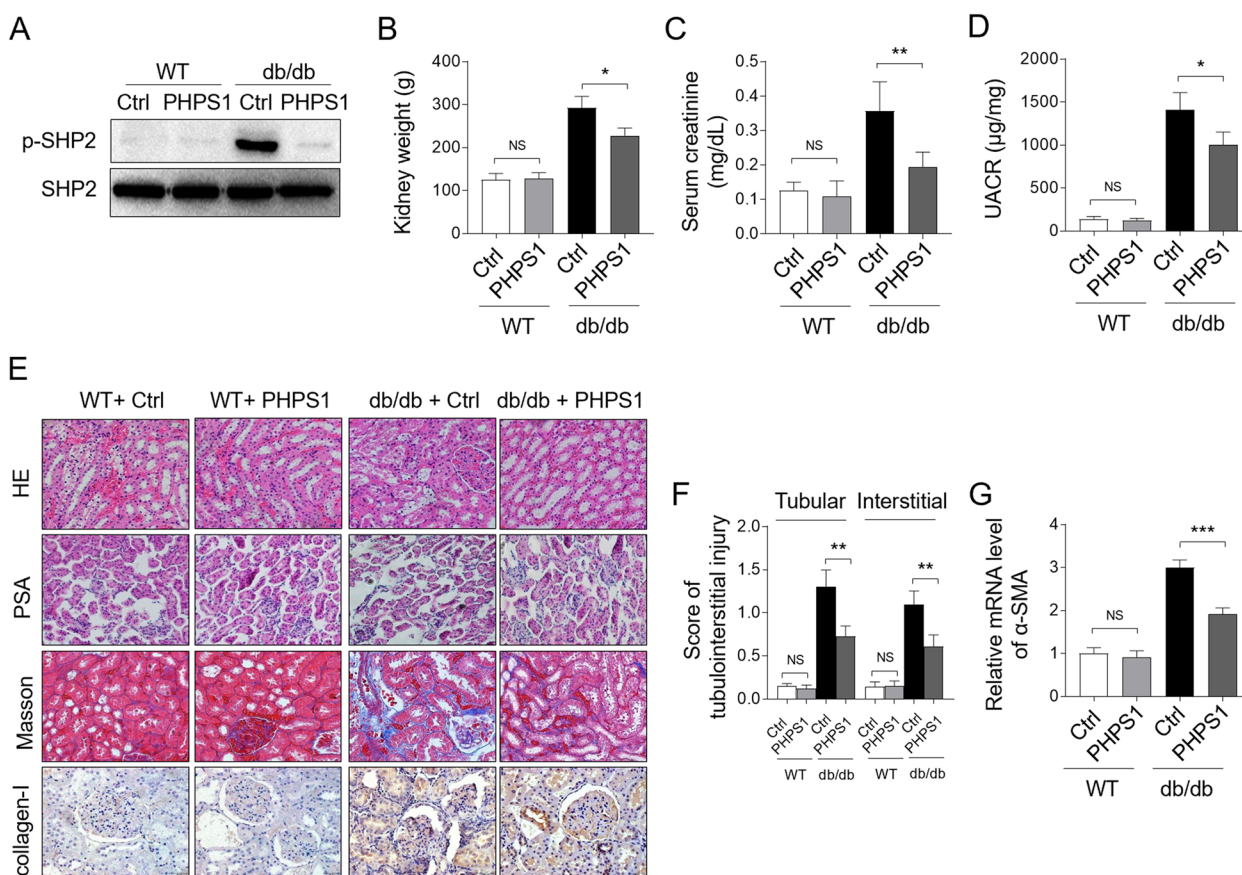


Fig. 3 PPHP51 alleviates renal injury in db/db mice. **A** WT and db/db mice were administered i.p. with 8 mg/kg/d PPHP51 for 12 weeks, starting at 8 weeks to 20 weeks of age. Injection of equal volume of vehicle was used as control (Ctrl). Each group included 6 mice. The levels of p-SHP2 and basal SHP2 protein were determined by Western blot analysis. **B-D** Mice were treated as in (A). Mouse kidneys in each group were harvested and weighed (B). The urinary albumin and creatinine levels were measured using enzyme-linked immunosorbent assay (ELISA), and the serum creatinine level (C) and urine albumin-to-creatinine ratio (UACR) (D) were presented. Student's test, *, $p < 0.05$; **, $p < 0.01$; NS, not significant ($n = 6$). **E** Histologic examinations of renal sections from each group were performed via hematoxylin and eosin (HE) staining and periodic acid-Schiff (PAS) staining. Masson trichrome staining and IHC staining of collagen-I were employed to measure collagen fiber deposition. **F** The tubulointerstitial injury in (E) was semiquantified and the score in each group was depicted. Student's test, **, $p < 0.01$; NS, not significant ($n = 6$). **G** The mRNA level of α -SMA in renal tissue was detected by qRT-PCR analysis. Student's test, ***, $p < 0.001$; NS, not significant ($n = 6$)

renal tubulointerstitial injuries were alleviated by PHPS1 treatment (Fig. 3E-F). Consistent with these histologic results, the elevated mRNA expression level of the profibrotic molecule alpha-smooth muscle actin (α -SMA) in the kidneys of db/db mice was distinctly prevented upon PHPS1 administration (Fig. 3G). Altogether, these observations suggest that SHP2 inhibition with PHPS1 is able to mitigate renal injury in db/db mice.

PHPS1 administration attenuates renal inflammation in db/db mice

It has been documented that SHP2 is able to regulate some inflammatory diseases [20]. In order to investigate whether the protective effect of SHP2 inhibition against renal injury in DN is attributed to its anti-inflammatory activities, we checked the levels of some important pro-inflammatory factors in the kidney tissue. qRT-PCR analysis manifested that the levels of the tumor necrosis factor- α (TNF- α) (Fig. 4A), interleukin (IL)-6 (Fig. 4B), as well as CC chemokine ligand (CCL)-2 (Fig. 4C) were all induced in db/db mice, whereas SHP2 inhibition with PHPS1 markedly reduced the level of these pro-inflammatory cytokines. IHC staining of renal sections also displayed that PHPS1 treatment prevented CCL-2 induction in db/db mice (Fig. 4D). In concert with these findings,

the percentage of F4/80⁺ macrophage infiltrated into the renal tissue was remarkably decreased by PHPS1 in the tubulointerstitium of db/db mice (Fig. 4D-E). In sum, these findings indicate that the along with alleviated renal injury, the renal inflammation in db/db mice mediated by proinflammatory factors is also dampened by SHP2 inhibition with PHPS1.

PHPS1 treatment inhibits high glucose-induced inflammatory responses in vitro

We next extended our findings in vitro using HK-2 cells, immortalized proximal tubule epithelial cells established from normal adult human kidney [21], which were exposed to high glucose (HG, 30mM) culture condition. We found that pre-treatment with PHPS1 prevented elevated production of proinflammatory cytokines by HG stimulation, including TNF- α (Fig. 5A), IL-6 (Fig. 5B), as well as CCL-2 (Fig. 5B), indicating that HG-induced inflammatory responses were repressed by PHPS1 treatment. In consistency with these findings, the activated proinflammatory pathway ERK/NF- κ B by high glucose exposure was hindered by PHPS1 in HK-2 cells, as shown by markedly reduced level of p-ERK and p-NF- κ B (Fig. 5D) and the corresponding decreased ratio of p-ERK/ERK (Fig. 5E) and p-NF- κ B/NF- κ B (Fig. 5F). Taken

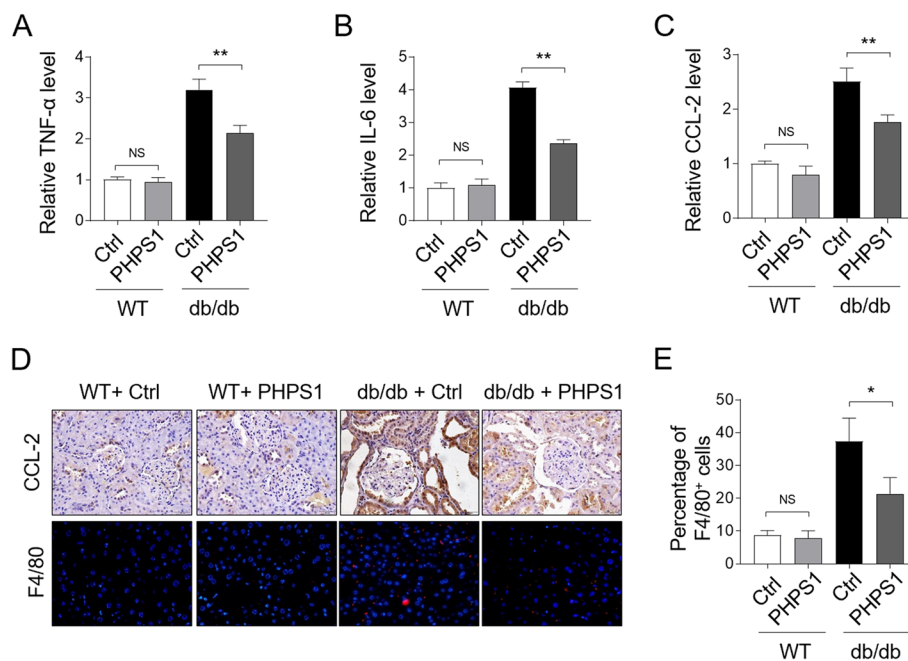


Fig. 4 PHPS1 alleviates renal inflammation in db/db mice. **A-C** WT and db/db mice were administered i.p. with 8 mg/kg/d PHPS1 for 12 weeks, starting at 8 weeks to 20 weeks of age. Injection of equal volume of vehicle was used as control (Ctrl). Each group included 6 mice. The mRNA level of TNF- α (**A**), IL-6 (**B**), and CCL-2 (**C**) in renal tissue of each group mice was quantified by qRT-PCR analysis. Student's test, **, $p < 0.01$; NS, not significant ($n = 6$). **D** CCL-2 in kidney tissue isolated from each group was stained by IHC experiment (upper). The immunofluorescent detection of F4/80 (red dots) was used to evaluate renal macrophage infiltration (lower). **E** The number of F4/80⁺ infiltrated macrophages as shown in (**D**) was quantified and the percentage of these cells in each group was presented. Student's test, *, $p < 0.05$; NS, not significant ($n = 6$)

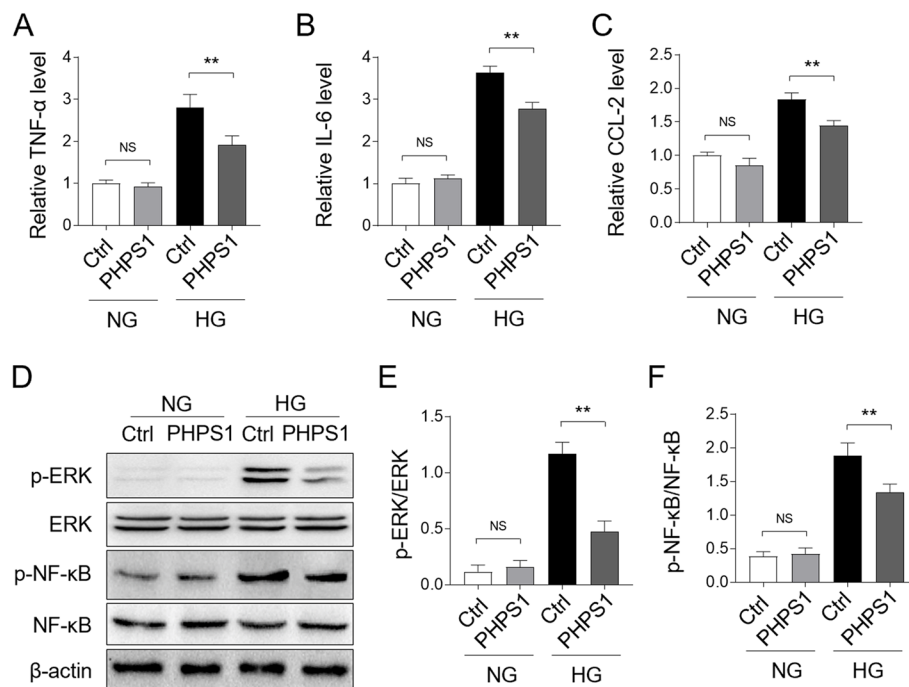


Fig. 5 PHPS1 decreases HG-induced inflammatory responses in HK-2 cells in vitro. **A-C** HK-2 cells were pretreated with 5 μ M PHPS1 before exposure to high glucose (HG, 30 mM) for 24 h. The control group was incubated with normal glucose (NG, 5.5 mM). The mRNA level of TNF- α (**A**), IL-6 (**B**), and CCL-2 (**C**) in each group of HK-2 cells was quantified by qRT-PCR analysis. Student's test, **, $p < 0.01$; NS, not significant ($n = 3$). **D-F** HK-2 cells were treated as in (A-C), the levels of p-ERK, p-NF- κ B and their basal protein expression were measured by Western blot analysis. The representative images were shown (**D**). The intensity of protein bands (**D**) was quantified by ImageJ and the ratio of p-ERK/ERK (**E**) and p-NF- κ B/NF- κ B (**F**) were depicted. Student's test, **, $p < 0.01$; NS, not significant ($n = 3$)

together, these results unveil that SHP2 inhibitor PHPS1 ameliorates high glucose-induced inflammation and blocks the activation of proinflammatory ERK/NF- κ B pathway in HK-2 cells.

PHPS1 prevents high glucose-induced inflammatory responses through suppressing ERK/NF- κ B pathway

The activation of ERK/NF- κ B pathway is important for mediating inflammation in a variety of settings [22–24]. In light of the above finding that the ERK/NF- κ B pathway was inhibited by PHPS1, we wondered whether this pathway accounted for the anti-inflammatory effect of PHPS1 in HK-2 cells. To test this idea, we pretreated HK-2 cells with a specific ERK pathway inhibitor PD98059 to eliminate the influence of this pathway on PHPS1 activity. As shown in Fig. 6A, PHPS1 treatment alone consistently attenuated TNF- α induction in HG-stimulated HK-2 cells, while combined treatment with PD98059 could no longer exert similar anti-inflammatory activity. Likewise, PHPS1 treatment led to no significant changes in the induction of IL-6 (Fig. 6B) and CCL-2 (Fig. 6C) in the presence of PD98059. These results describe that

PHPS1-prevented inflammatory responses rely on inhibited ERK pathway. This notion was further strengthened by the evidence that PHPS1 failed to restrict the activation of ERK/NF- κ B pathway in combination with PD98059 pretreatment, compared with PHPS1 treatment alone, as shown by Western blot analysis (Fig. 6D) and the ratio of p-ERK/ERK (Fig. 6E) and p-NF- κ B/NF- κ B (Fig. 6F). Hence, the ERK/NF- κ B pathway regulates the anti-inflammatory effect of PHPS1 on HK-2 cells exposed to HG.

PHPS1 limits ERK/NF- κ B activation in db/db mice

To establish a causal link between protective activity of PHPS1 against renal injury and ERK/NF- κ B pathway modulation, we then examined whether PHPS1 inhibits ERK/NF- κ B pathway in vivo. Through checking the phosphorylated proteins via Western blot analysis on kidney tissue samples, we noticed that along with the decreased level of p-SHP2 in db/db mice by PHPS1 administration, the levels of p-ERK and p-NF- κ B were accordingly downregulated (Fig. 7A). To verify this, we further detected the expression of these phosphorylated proteins

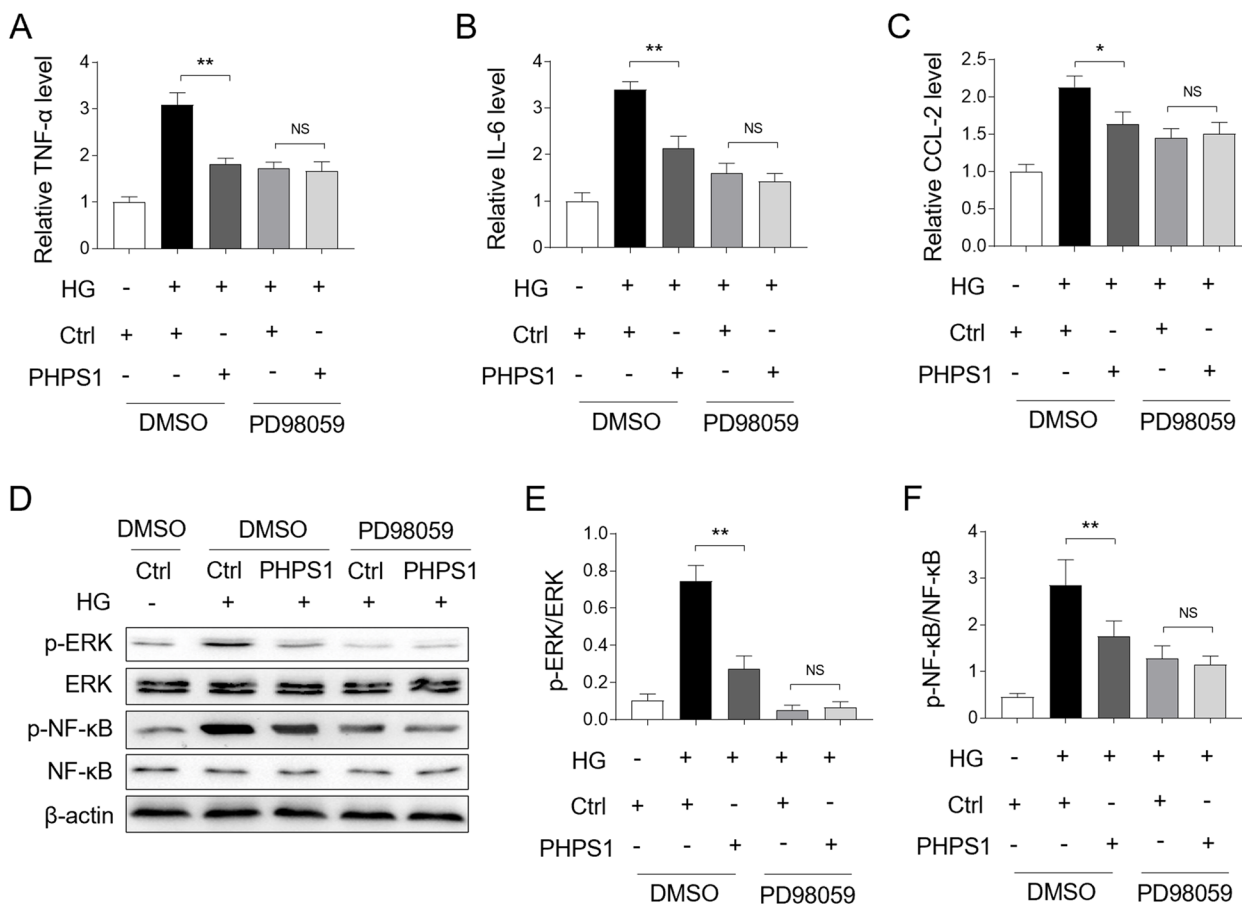


Fig. 6 PHPS1 prevents high glucose-induced inflammatory responses through ERK/NF-κB pathway. **A-C** HK-2 cells were pretreated with 5 μM PHPS1 alone or in combination with 50 μM PD98059 before exposure to high glucose (HG, 30 mM) for 24 h. The control group was incubated with normal glucose (NG, 5.5 mM). The mRNA level of TNF-α (**A**), IL-6 (**B**), and CCL-2 (**C**) in each group of HK-2 cells was quantified by qRT-PCR analysis. Student's test, **, $p < 0.01$; *, $p < 0.05$; NS, not significant ($n = 3$). **D-F** HK-2 cells were treated as in (A-C), the levels of p-ERK, p-NF-κB and their basal protein expression were measured by Western blot analysis. The representative images were shown (**D**). The intensity of protein bands (**D**) was quantified by ImageJ and the ratio of p-ERK/ERK (**E**) and p-NF-κB/NF-κB (**F**) were depicted. Student's test, **, $p < 0.01$; NS, not significant ($n = 3$)

in kidney sections by IHC assay, and similar tendency was obtained, as indicated by significantly reduced levels of p-SHP2 (Fig. 7B and C), p-ERK (Fig. 7B and D), and p-NF-κB (Fig. 7B and E) in db/db mice administrated with PHPS1. Therefore, PHPS1 also negatively regulates the activation of ERK/NF-κB pathway in db/db mice.

SHP2 activation correlates positively with ERK/NF-κB activation in DN patients

To understand the relation of the activation status of SHP2 and ERK/NF-κB pathway in human DN pathology, we performed immunostaining of p-SHP2, p-ERK and p-NF-κB on human DN samples through IHC (Fig. 8A), and further analyzed the correlation between their expression levels. The results illustrated that p-SHP2 level was positively associated with that of p-ERK (Fig. 8B) and p-NF-κB (Fig. 8C). Moreover, consistent with these,

immunohistochemical staining of CD3⁺ (T lymphocytes) and chemokine (C-C motif) ligand 2/monocyte chemoattractant protein-1 (CCL-2/MCP-1) in the kidney showed that their expression was much more pronounced in DN kidney sections than in the normal kidney sections (Supplementary Fig. 2). Based on the above observations that SHP2 inhibition with PHPS1 limited ERK/NF-κB activation and suppressed inflammation in db/db mice and in vitro condition, these results together imply that the activation of SHP2 positively regulates the ERK/NF-κB pathway to induce renal inflammation in DN, whereby promoting disease progression and renal injury.

Discussion

Increasing studies have demonstrated an important role of inflammation in DN pathogenesis and renal damage, however the involved regulatory factors and underlying

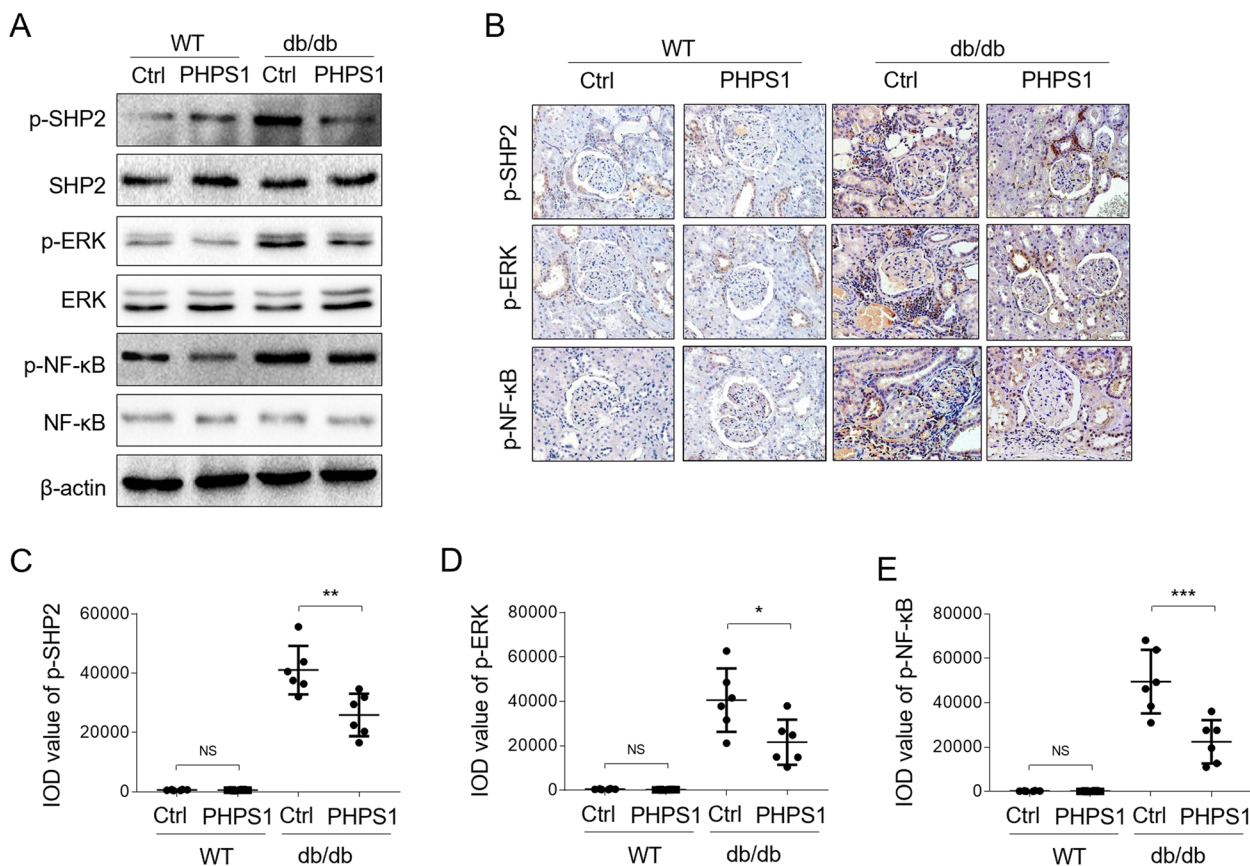


Fig. 7 ERK/NF-κB pathway is constrained by PHPS1 in db/db mice. **A** WT and db/db mice were administered i.p. with 8 mg/kg/d PHPS1 for 12 weeks, starting at 8 weeks to 20 weeks of age. Injection of equal volume of vehicle was used as control (Ctrl). Each group included 6 mice. The levels of p-SHP2, p-ERK, p-NF-κB and their basal proteins were determined by Western blot analysis, and the representative images were shown. **B** Immunostaining of p-SHP2, p-ERK, p-NF-κB on mouse normal kidney sections ($n=6$) and kidney biopsy samples of db/db mice ($n=6$) was detected by IHC experiment. **C-E** The integrated optical density (IOD) of expression of p-SHP2 (**C**), p-ERK (**D**), and p-NF-κB (**E**) was shown. Student's test, ***, $p < 0.001$; **, $p < 0.01$; *, $p < 0.05$

mechanisms are not fully clear. In the current study, we provided some lines of evidence in the first time revealing that the activity of a cytosolic protein tyrosine phosphatase, i.e., SHP2, was enhanced in kidney biopsies of DN patients as well as db/db mice. Through a pharmacological inhibition strategy of SHP2 using PHPS1 administered in an animal model of DN, we demonstrated that inhibiting SHP2 activity yielded therapeutic effects on alleviating renal injury and attenuating renal inflammation in vivo, hence offering SHP2 as a new potential target in DN therapy. To gain molecular insights into the SHP2 regulation of inflammation, we elucidated the signaling pathway through which SHP2 regulates inflammation in HK-2 cells stimulated by high glucose in vitro, and discovered that SHP2 inhibition by PHPS1 prevented high glucose-induced inflammatory responses through suppressing the proinflammatory ERK/NF-κB pathway. More importantly, in accordance with this molecular

mechanism, the activation of ERK/NF-κB pathway was similarly suppressed by PHPS1 in db/db mice in vivo, and histologic examinations of human DN samples further revealed a positive correlation between SHP2 activity and ERK/NF-κB activation. In conclusion, our study reports a therapeutic effect of pharmacological targeting of SHP2 on renal injury in an animal DN model, and also highlights a critical role of SHP2/ERK/NF-κB pathway-induced production of proinflammatory cytokines and -elicited inflammation in promoting renal injury in DN pathology (Fig. 9).

SHP2 is a protein tyrosine phosphatase widely expressed in most tissues and cells and functions to regulate cytokine, integrin, and tyrosine receptor signaling pathways. Its aberration has a causal link to multiple diseases including systemic lupus erythematosus, cancer, and other genetic disorders [25–28]. Studies have also shown that SHP2 can regulate some inflammatory

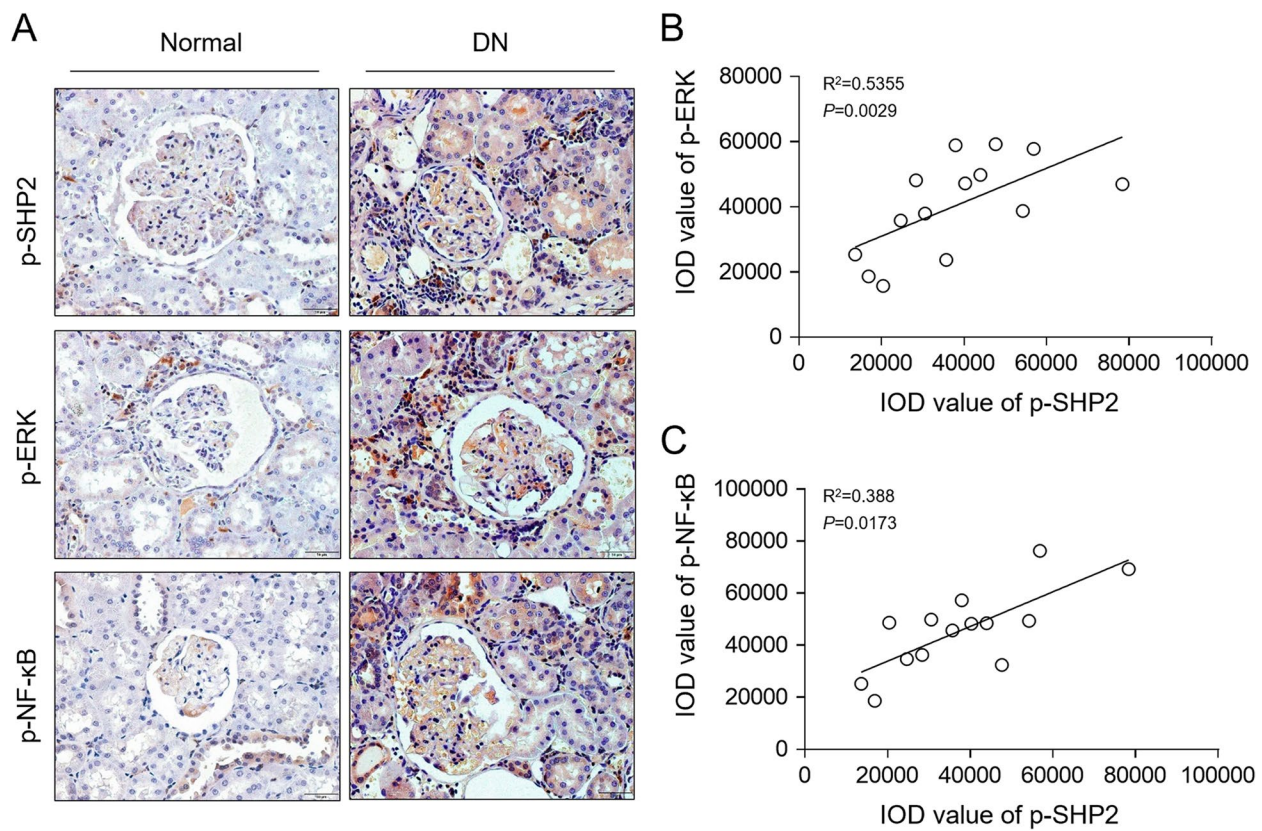


Fig. 8 SHP2 activation correlates positively with ERK/NF-κB activation in DN patients. **A** Immunostaining of p-SHP2, p-ERK and p-NF-κB on kidney biopsy samples of DN patients ($n=14$) was visualized by IHC experiment. **B, C** Correlation analysis of integrated optical density (IOD) of p-SHP2 expression with that of p-ERK (**B**) and p-NF-κB (**C**). Pearson's correlation analysis

diseases, such as cancer-related inflammation and metabolic diseases [20]. We found that the activity of SHP2 was induced in DN without the change of its expression level, which extends its scope of functions involved in inflammatory and metabolic diseases. However, the upstream regulator(s) activating SHP2 are unclear. SHP2 activation can be regulated by different receptor tyrosine kinases (RTKs), which recruit SHP2 to the plasma membrane for its activation in response to cellular signals, for example the stimulation of cytokines [29]. Within the local pro-inflammatory niche of injured kidney tissue with DN, inflammatory cells infiltrate the site of injury and result in profibrotic cytokine pressure [30], it may thus be plausible that the observed activation of SHP2 in DN is at least partly attributed to stimulation of RTKs by local cytokines. Besides, studies have shown that the protein tyrosine kinases (PTKs) can also regulate SHP2 activity through multiple signaling pathways [31, 32], making the regulation network of SHP2 highly complicated. Further investigations on seeking SHP2 activator(s) in DN scenario are needed.

PHPS1 was identified as an active site-directed small molecule inhibitor of SHP2 in 2008 [19]. Since its discovery, PHPS1 has been demonstrated to show ameliorating effect in multiple diseases in animal models, such as acute kidney injury [33], atherosclerosis [34], cardiac hypertrophy [35], pulmonary arterial hypertension [36], and systemic lupus erythematosus [25]. In our study, PHPS1 treatment via i.p. injection alleviated renal injury and exerted anti-inflammatory activity in db/db mice, hence suggesting it as a promising therapeutic in DN treatment. Together with previous studies mentioned above, these findings support a wide spectrum of PHPS1 utility in the treatment of SHP2-related human diseases.

The ERK/NF-κB pathway is a well-established proinflammatory pathway responsible for proinflammatory cytokine production and inflammation initiation [22, 37–41]. In addition, two earlier studies have shown that SHP2 phosphorylation is critical for ERK activation in response to growth factors by controlling Csk recruitment [15, 16]. Consistent with these hints, we found that SHP2 inhibition suppressed ERK/NF-κB pathway

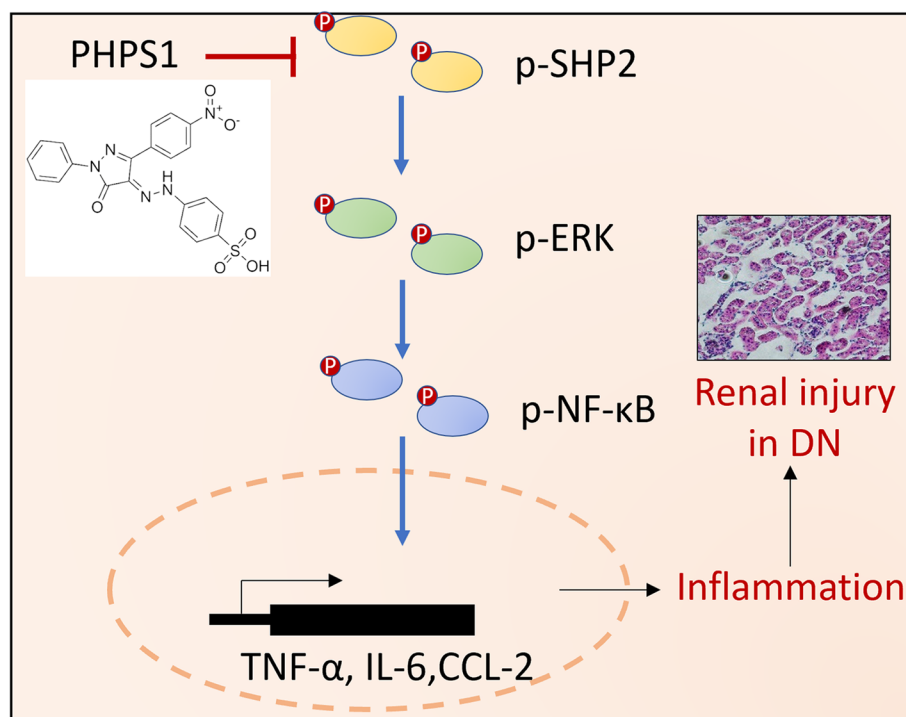


Fig. 9 Schematic diagram illustrating the mechanism of action of the therapeutic effect of PHS1 in DN. PHS1 inhibition of SHP2 activity ameliorates renal injury in DN by attenuating ERK/NF-κB pathway-mediated inflammation

activation, and further confirmed its important role in limiting proinflammatory responses in HK-2 cells and in db/db mice. These results connect SHP2 activity to regulation of downstream ERK/NF-κB pathway status which plays an unprecedented role in renal inflammation in DN pathogenesis. However, it should be noted that ERK and NF-κB are not the sole effectors downstream SHP2 kinase, and other biological effects of SHP2 inhibition with PHS1 on DN can not be ruled out and remain uncertain, which requires further studies.

Supplementary Information

The online version contains supplementary material available at <https://doi.org/10.1186/s12964-023-01394-9>.

Additional file 1: Fig. S1. The parameters of mice used in this study. The blood glucose levels (A) and body weight (B) of the WT and db/db mice were measured every 2 weeks. Each group included 6 mice. One-way ANOVA test followed by a Holm-Sidak post-test, **, $p < 0.01$.

Additional file 2: Fig. S2. Correlation between SHP2 activity and inflammation degree in DN patients. Correlation analysis of integrated optical density (IOD) of p-SHP2 expression with that of CD3⁺ (A) and CCL2 (B). Pearson's correlation analysis.

Acknowledgments

Not applicable.

Authors' contributions

Conceptualization, Che Yu; Experiments and Formal analysis, CuiLi Nie, Lei Chang; Funding acquisition, Zhuo Li; Investigation, Tao Jiang; Methodology,

Che Yu and Zhuo Li; Writing—original draft, Che Yu; Review & editing, Tao Jiang. All authors have read and agreed to the published version of the manuscript.

Funding

This research was supported by the Shandong Natural Science Foundation Youth Program (ZR2022QH323).

Availability of data and materials

The datasets generated and/or used during the present study are available from the corresponding author upon reasonable request.

Declarations

Ethics approval and consent to participate

The study was reviewed and approved by Ethics Committee of Provincial Hospital Affiliated to Shandong First Medical University (NO.SD NSFC 2021-0168).

Competing interests

The authors declare no competing interests.

Received: 27 June 2023 Accepted: 11 November 2023

Published online: 18 December 2023

References

- Sagoo MK, Gnudi L. Diabetic nephropathy: an overview. *Methods Mol Biol.* 2020;2067:3–7.
- Tang G, Li S, Zhang C, Chen H, Wang N, Feng Y. Clinical efficacies, underlying mechanisms and molecular targets of Chinese medicines for diabetic nephropathy treatment and management. *Acta Pharm Sin B.* 2021;11:2749–67.

3. Natesan V, Kim SJ. Diabetic nephropathy - a review of risk factors, progression, mechanism, and dietary management. *Biomol Ther (Seoul)*. 2021;29:365–72.
4. Agarwal R. Pathogenesis of Diabetic Nephropathy. *Compendia*. 2021;2021:2–7.
5. Rayego-Mateos S, Morgado-Pascual JL, Opazo-Rios L, Guerrero-Hue M, Garcia-Caballero C, Vazquez-Carballo C, Mas S, Sanz AB, Herencia C, Mezzano S, et al. Pathogenic pathways and therapeutic approaches targeting inflammation in diabetic nephropathy. *Int J Mol Sci*. 2020;21:3798.
6. Donate-Correa J, Luis-Rodriguez D, Martin-Nunez E, Tagua VG, Hernandez-Carballo C, Ferri C, Rodriguez-Rodriguez AE, Mora-Fernandez C, Navarro-Gonzalez JF. Inflammatory Targets in Diabetic Nephropathy. *J Clin Med*. 2020;9:458.
7. Chen YN, LaMarche MJ, Chan HM, Fekkes P, Garcia-Fortanet J, Acker MG, Antonakos B, Chen CH, Chen Z, Cooke VG, et al. Allosteric inhibition of SHP2 phosphatase inhibits cancers driven by receptor tyrosine kinases. *Nature*. 2016;535:148–52.
8. Lauriol J, Jaffre F, Kontaridis MI. The role of the protein tyrosine phosphatase SHP2 in cardiac development and disease. *Semin Cell Dev Biol*. 2015;37:73–81.
9. Giri H, Muthuramu I, Dhar M, Rathnakumar K, Ram U, Dixit M. Protein tyrosine phosphatase SHP2 mediates chronic insulin-induced endothelial inflammation. *Arterioscler Thromb Vasc Biol*. 2012;32:1943–50.
10. Dorenkamp M, Muller JP, Shanmuganathan KS, Schulten H, Muller N, Loffler I, Muller UA, Wolf G, Bohmer FD, Godfrey R, Waltenberger J. Hyperglycaemia-induced methylglyoxal accumulation potentiates VEGF resistance of diabetic monocytes through the aberrant activation of tyrosine phosphatase SHP-2/SRC kinase signalling axis. *Sci Rep*. 2018;8:14684.
11. Dorenkamp M, Nasiry M, Koch S, Semo D, Loeffler I, Wolf G, Reinecke H, Godfrey R. Inflammatory and diabetic conditions trigger SHP2 tyrosine phosphatase expression and subsequent aberrant activation of primary human monocytes. *Eur Heart J*. 2022;43:3081–3081.
12. Dorenkamp M, Nasiry M, Semo D, Koch S, Loffler I, Wolf G, Reinecke H, Godfrey R. Pharmacological targeting of the RAGE-NFkappaB Signalling Axis impedes monocyte activation under diabetic conditions through the repression of SHP-2 tyrosine phosphatase function. *Cells*. 2023;12:513.
13. Hu Y, Wang SX, Wu FY, Wu KJ, Shi RP, Qin LH, Lu CF, Wang SQ, Wang FF, Zhou S. Effects and mechanism of Ganoderma lucidum polysaccharides in the treatment of diabetic nephropathy in Streptozotocin-induced diabetic rats. *Biomed Res Int*. 2022;2022:4314415.
14. Ye Z, Zhang C, Tu T, Sun M, Liu D, Lu D, Feng J, Yang D, Liu F, Yan X. Wnt5a uses CD146 as a receptor to regulate cell motility and convergent extension. *Nat Commun*. 2013;4:2803.
15. Araki T, Nawa H, Neel BG. Tyrosyl phosphorylation of Shp2 is required for normal ERK activation in response to some, but not all, growth factors. *J Biol Chem*. 2003;278:41677–84.
16. Zhang SQ, Yang W, Kontaridis MI, Bivona TG, Wen G, Araki T, Luo J, Thompson JA, Schraven BL, Philips MR, Neel BG. Shp2 regulates SRC family kinase activity and Ras/Erk activation by controlling Csk recruitment. *Mol Cell*. 2004;13:341–55.
17. Ahmed TA, Adamopoulos C, Karoulia Z, Wu X, Sachidanandam R, Aaronson SA, Poulikakos PI. SHP2 drives adaptive resistance to ERK signaling inhibition in molecularly defined subsets of ERK-dependent tumors. *Cell Rep*. 2019;26(65–78):e65.
18. Alpers CE, Hudkins KL. Mouse models of diabetic nephropathy. *Curr Opin Nephrol Hypertens*. 2011;20:278–84.
19. Hellmuth K, Grosskopf S, Lum CT, Wurtele M, Roder N, von Kries JP, Rosario M, Rademann J, Birchmeier W. Specific inhibitors of the protein tyrosine phosphatase Shp2 identified by high-throughput docking. *Proc Natl Acad Sci U S A*. 2008;105:7275–80.
20. Liu Y, Yang X, Wang Y, Yang Y, Sun D, Li H, Chen L. Targeting SHP2 as a therapeutic strategy for inflammatory diseases. *Eur J Med Chem*. 2021;214:113264.
21. Ryan MJ, Johnson G, Kirk J, Fuerstenberg SM, Zager RA, Torok-Storb B. HK-2: an immortalized proximal tubule epithelial cell line from normal adult human kidney. *Kidney Int*. 1994;45:48–57.
22. Zhi L, Ang AD, Zhang H, Moore PK, Bhatia M. Hydrogen sulfide induces the synthesis of proinflammatory cytokines in human monocyte cell line U937 via the ERK-NF-kappaB pathway. *J Leukoc Biol*. 2007;81:1322–32.
23. Xie S, Liu B, Fu S, Wang W, Yin Y, Li N, Chen W, Liu J, Liu D. GLP-2 suppresses LPS-induced inflammation in macrophages by inhibiting ERK phosphorylation and NF-kappaB activation. *Cell Physiol Biochem*. 2014;34:590–602.
24. Zhang Q, Liu L, Hu Y, Shen L, Li L, Wang Y. Kv1.3 channel is involved in ox-LDL-induced macrophage inflammation via ERK/NF-kappaB signaling pathway. *Arch Biochem Biophys*. 2022;730:109394.
25. Wang J, Mizui M, Zeng LF, Bronson R, Finnell M, Terhorst C, Kyttaris VC, Tsokos GC, Zhang ZY, Kontaridis MI. Inhibition of SHP2 ameliorates the pathogenesis of systemic lupus erythematosus. *J Clin Invest*. 2016;126:2077–92.
26. Song Y, Wang S, Zhao M, Yang X, Yu B. Strategies targeting protein tyrosine phosphatase SHP2 for Cancer therapy. *J Med Chem*. 2022;65:3066–79.
27. Mohi MG, Williams IR, Dearolf CR, Chan G, Kutok JL, Cohen S, Morgan K, Boulton C, Shigematsu H, Keilhack H, et al. Prognostic, therapeutic, and mechanistic implications of a mouse model of leukemia evoked by Shp2 (PTPN11) mutations. *Cancer Cell*. 2005;7:179–91.
28. Li SM. The biological function of SHP2 in human disease. *Mol Biol (Mosk)*. 2016;50:27–33.
29. Matakah F, Martin E, Zhao H, Agazie YM. SHP2 acts both upstream and downstream of multiple receptor tyrosine kinases to promote basal-like and triple-negative breast cancer. *Breast Cancer Res*. 2016;18:2.
30. Kanasaki K, Taduri G, Koya D. Diabetic nephropathy: the role of inflammation in fibroblast activation and kidney fibrosis. *Front Endocrinol (Lausanne)*. 2013;4:7.
31. Cha Y, Park KS. SHP2 is a downstream target of ZAP70 to regulate JAK1/STAT3 and ERK signaling pathways in mouse embryonic stem cells. *FEBS Lett*. 2010;584:4241–6.
32. Burmeister BT, Wang L, Gold MG, Skidgel RA, O'Bryan JP, Carnegie GK. Protein kinase A (PKA) phosphorylation of Shp2 protein inhibits its phosphatase activity and modulates ligand specificity. *J Biol Chem*. 2015;290:12058–67.
33. Jiang J, Hu B, Chung CS, Chen Y, Zhang Y, Tindal EW, Li J, Ayala A. SHP2 inhibitor PHS1 ameliorates acute kidney injury by Erk1/2-STAT3 signaling in a combined murine hemorrhage followed by septic challenge model. *Mol Med*. 2020;26:89.
34. Chen J, Cao Z, Guan J. SHP2 inhibitor PHS1 protects against atherosclerosis by inhibiting smooth muscle cell proliferation. *BMC Cardiovasc Disord*. 2018;18:72.
35. Schramm C, Edwards MA, Crombie K, Krenz M. Abstract 15204: inhibition of Shp2's phosphatase activity ameliorates cardiac hypertrophy in LEOP-ARD syndrome models. *Circulation*. 2013;128:A15204–4.
36. Cheng Y, Yu M, Xu J, He M, Wang H, Kong H, Xie W. Inhibition of Shp2 ameliorates monocrotaline-induced pulmonary arterial hypertension in rats. *BMC Pulm Med*. 2018;18:130.
37. Zhang H, Wang ZW, Wu HB, Li Z, Li LC, Hu XP, Ren ZL, Li BJ, Hu ZP. Transforming growth factor-beta1 induces matrix metalloproteinase-9 expression in rat vascular smooth muscle cells via ROS-dependent ERK-NF-kappaB pathways. *Mol Cell Biochem*. 2013;375:11–21.
38. Jung YC, Kim ME, Yoon JH, Park PR, Youn HY, Lee HW, Lee JS. Anti-inflammatory effects of galangin on lipopolysaccharide-activated macrophages via ERK and NF-kappaB pathway regulation. *Immunopharmacol Immunotoxicol*. 2014;36:426–32.
39. Zhong X, Li X, Liu F, Tan H, Shang D. Omentin inhibits TNF-alpha-induced expression of adhesion molecules in endothelial cells via ERK/NF-kappaB pathway. *Biochem Biophys Res Commun*. 2012;425:401–6.
40. Xia L, Tian D, Huang W, Zhu H, Wang J, Zhang Y, Hu H, Nie Y, Fan D, Wu K. Upregulation of IL-23 expression in patients with chronic hepatitis B is mediated by the HBx/ERK/NF-kappaB pathway. *J Immunol*. 2012;188:753–64.
41. Chan LP, Liu C, Chiang FY, Wang LF, Lee KW, Chen WT, Kuo PL, Liang CH. IL-8 promotes inflammatory mediators and stimulates activation of p38 MAPK/ERK-NF-kappaB pathway and reduction of JNK in HNSCC. *Oncotarget*. 2017;8:56375–88.

Publisher's Note

Springer Nature remains neutral with regard to jurisdictional claims in published maps and institutional affiliations.